REPORT DOCUMENTATION PAGE

AFRL-SR-AR-TR-03-

0093

1. AGENCY USE ONLY *(Leave blank)*	2. REPORT DATE	3. [illegible] AND DATES COVERED
	17 MAR 03	FINAL REPORT - 01 JAN 00 TO 30 NOV 02

4. TITLE AND SUBTITLE
CHARACTERIZATION AND IMPROVEMENT OF POLYMER SOLUTION LIGHT-EMITTING DEVICES

5. FUNDING NUMBERS
F49620-00-1-0103
2303/CV
61102F

6. AUTHOR(S)
PROF. YANG YANG

7. PERFORMING ORGANIZATION NAME(S) AND ADDRESS(ES)
UNIVERSITY OF CALIFORNIA, LOS ANGELES
DEPARTMENT OF MATERIALS SCIENCE AND ENGINEERING
6531 BOELTER HALL
LOS ANGELES, CA 90095

8. PERFORMING ORGANIZATION REPORT NUMBER

9. SPONSORING/MONITORING AGENCY NAME(S) AND ADDRESS(ES)
AFOSR/NL
4015 WILSON BLVD. ROOM 713
ARLINGTON, VA 22203-1954

10. SPONSORING/MONITORING AGENCY REPORT NUMBER

11. SUPPLEMENTARY NOTES

12a. DISTRIBUTION AVAILABILITY STATEMENT
Approve for Public Release: Distribution Unlimited

20030508 151

13. ABSTRACT *(Maximum 200 words)*

Our original objective was the understanding of polymer solution ligh-emitting devices (SLED), from device mechanism to materials. After a two-year intense research on SLEDs, we have expanded our project to other areas, from SLEDs, to phosphorescent PLEDs, and high performance photovoltaic devices. It is realized that our SLED has a similar mechanism as the ECL process. The electrogenerated chemiluminescence (ECL) process usually involves at least two species (or two reactions). One reaction is the oxidation process in which a species is oxidized near the anode to form a radical cation and the other species is reduced near the cathode to form a radical anion. The radical species with lower molecular weight will move to the counter-electrode. When the radical anions and radical cations encounter within the charge hopping distance, charge ransfer will occur. The electron transition is from the high-energy excited state (Eex) to the low-energy state. In the case of poly [9,9-bis(3,6-dioxaheptyl)-fluorene-2,7-diyl] (BDOH-PF) and 1,2-dichlorobenzene (DCB), Eex(BDOH-PF < Eex(DCB) and the radical cation of DCB will transfer its positive charge to the radical anions of BDOH-PF (actually an electron hops from the radical anion to the DCB radical cation) to form the excited state of BDOH-PF and blue light emission will take place when the excited state decays to its ground state.

14. SUBJECT TERMS			15. NUMBER OF PAGES
			16. PRICE CODE
17. SECURITY CLASSIFICATION OF REPORT	18. SECURITY CLASSIFICATION OF THIS PAGE	19. SECURITY CLASSIFICATION OF ABSTRACT	20. LIMITATION OF ABSTRACT
UNCLAS	UNCLAS	UNCLAS	

Final Technical Report to AFOSR

Project title: Characterization and improvement of polymer solution light-emitting devices.

Grant Number: F49620-00-1-0103

Program Director: Dr. Charles Lee

PI: Prof. Yang Yang
Department of Materials Science and Engineering
UCLA
6531 Boelter Hall
Los Angeles, CA 90095

Co-PI: Prof. Fred Wudl
Dept. of Chemistry and Biochemistry
UCLA
Los Angeles, CA 90095

March 3, 2003

Objectives:

Our original objective was the understanding of polymer solution light-emitting devices (SLED), from device mechanism to materials. After a two-year intense research on SLEDs, we have expanded our project to other areas, from SLEDs, to phosphorescent PLEDs, and high performance photovoltaic devices.

Accomplishments

SLED mechanism study and improvements (First Year)

It is realized that our SLED has a similar mechanism as the ECL process. The electrogenerated chemiluminescence (ECL) process usually involves at least two species (or two reactions). One reaction is the oxidation process in which a species is oxidized near the anode to form a radical cation and the other species is reduced near the cathode to form a radical anion. The radical species with lower molecular weight will move to the counter-electrode. When the radical anions and radical cations encounter within the charge hopping distance, charge transfer will occur. The electron transition is from the high-energy excited state (E_{ex}) to the low-energy state. In the case of poly [9,9-bis(3,6-dioxaheptyl)-fluorene-2,7-diyl] (BDOH-PF) and 1,2-dichlorobenzene (DCB), E_{ex}(BDOH-PF) < E_{ex}(DCB) and the radical cation of DCB will transfer its positive charge to the radical anions of BDOH-PF (actually an electron hops from the radical anion to the DCB radical cation) to form the excited state of BDOH-PF and blue light emission will take place when the excited state decays to its ground state. Thus the mechanism can be expressed as the following.

Cathode: $PF + e^- \rightarrow PF^{-\bullet}$

Anode: $DCB + h^+ \rightarrow DCB^{+\bullet}$

Recombination: $PF^{-\bullet} + DCB^{+\bullet} \rightarrow DCB + PF^* \rightarrow DCB + PF + h\nu$

where PF is the BDOH-PF, DCB is the solvent molecule and hν is the emitted photon from BDOH-PF. This process was supported by our CV measurement shown in Fig. 1.

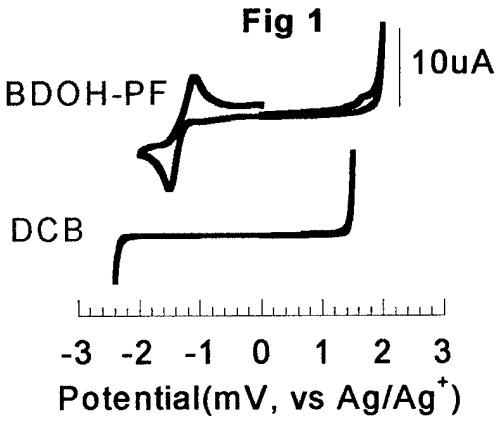

Figure 1. The CV measurement results from BDOH-PF and DCB.

Since the ECL is a kinetic-controlled process, the device operating temperature and the electrodes separation distance will play an important role to determine the reaction speed and, subsequently, influence the device performance. SLEDs, with 5% of BDOH-PF solution in DCB as the active medium were operated at different operating temperatures (15° and 45°C respectively), Fig. 2a and 2b show the corresponding L-V and I-V curves. The device turn-on voltage increased with a decrease in the operation temperature, as shown in Fig. 2a, which is in agreement with the ECL mechanism because the radical ions move slower at a lower temperature. Fig. 2b shows that current decreases when the device temperature is decreased, due to lower radical ion mobility at lower temperature. Fig. 3a shows the L-V curves of SLEDs with 1 μm, and 100 μm electrode separations at a constant voltage scan rate. Obviously, the device turn-on voltage increased with the increase of the solution layer thickness, which again agrees well with the ECL mechanism because longer time is needed for the radical ions to move through a thicker solution layer before producing ECL emission. The I-V curves of a device consisting of 5% BDOH-PF in DCB in Fig. 3b show that the currents decrease with increasing thickness of the solution layer, due to higher device resistance for thicker devices.

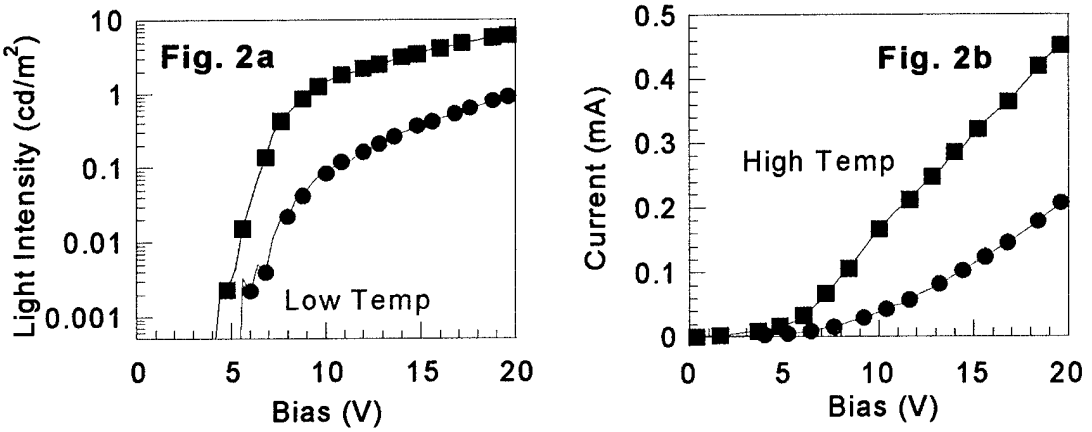

Figure 2a and Figure 2b show the difference of L-V and I-V curves for SLED operated under different operating temperature.

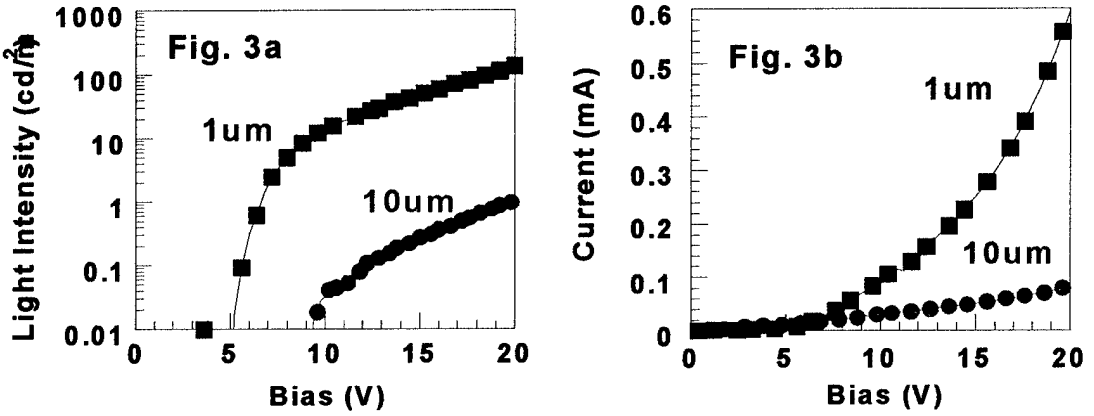

Figure 3a and Figure 3b show the difference of L-V and I-V curves for SLED operated under different operating thickness. At wider gap, the device show a much lower conductivity.

In addition to the CV measurement, electrochemical impedance spectroscopy was also applied to our investigation. It not only provides data on electrode capacitance and charge-transfer kinetics but also allows one to use a purely electronic model to represent an electrochemical cell, thus we applied an AC impedance technique to SLED to study the electrical behavior of the bulk and interfaces between polymer solution and electrodes. Fig. 4 shows the impedance plots (Nyquist plots) of the Imaginary part (Z") to Real part (Z') of the SLED device at different voltages from 0 V to 4 V. At zero bias (without bias), there is a semicircle in the high frequency range, whose diameter corresponds to the respective resistance, and a straight line, almost perpendicular to the Z' axis, in its lower frequency range. The impedance can be simulated by an equivalent circuit as shown in Fig. 5. The equivalent circuit is also based on the

structure of the SLED. In the equivalent circuit, C_1 represents the device capacitance, R_1 represents the resistance of the solution layer in the device, C_2 and R_2 represent the capacitance and resistance of the interface between the ITO electrodes and the solution layer respectively. C_2 should be much larger than C_1 due to the thinner width of the interface. The semicircle in the high frequency range should correspond to the parallel circuit of C_1 and R_1 because the impedance of the capacitor C_2 can be neglected at the high frequencies due to its high capacitance [$Z=-j(1/2\pi fC)$ for a capacitor C]. R_1, calculated from the semicircle in Fig. 4, is ca. 2 kΩ. In the lower frequency range, the impedance of C_1 in Fig. 4 is very large because of its very low capacitance, so that the circuit branch of C_1 behaves like an open circuit and the equivalent circuit becomes R_1 in series with the parallel C_2 and R_2. The straight line, almost perpendicular to the Z' axis, indicates that R_2 is very large at 0 V bias voltage.

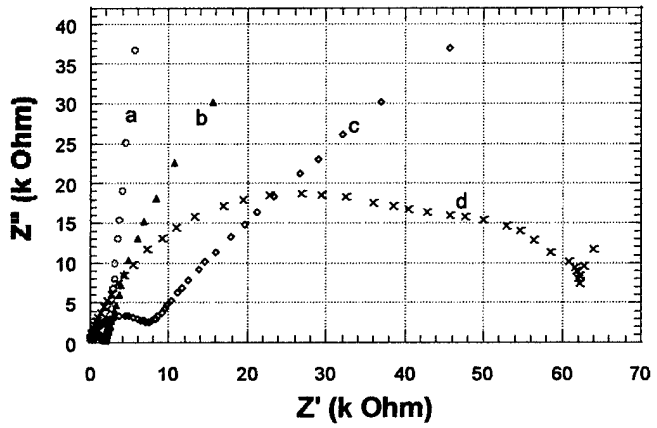

Fig. 4 shows the Nyquist plots of the Imaginary part (Z") to Real part (Z') of the SLED device at different voltages from 0 V to 4 V.

To analyze the capacitance values, Bode plots of log (Z") to log (*f*) (where *f* is frequency) were drawn in Fig. 6. In the plot without bias, there are two straight lines with the slope of ca.–1 in the high and low frequency range respectively. From the two straight lines, C_1 = 0.3 n F and C_2 = 200 n F were obtained. The value of 0.3 n F of C_1 is reasonable in comparison with ca. 2 n F for the solid polymer LEDs because the thickness of the SLED is ca. 2 μm, which is ca 10 times that of a polymer LED. In order to further verify that the values of C_1 and R_1 obtained in this way are the device capacitance and the solution layer resistance, we measured the ac

impedance of the SLED devices with different thickness of its solution layer. We can expect that R_1 will increase and C_1 will decrease with an increase in the device thickness.

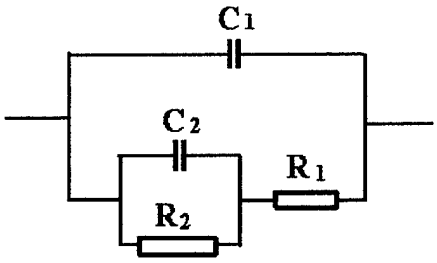

Fig 5 shows equivalent circuit of the simulation of SLED.

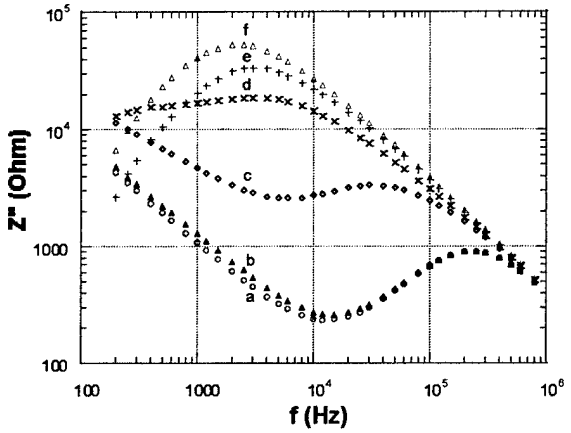

Fig. 6 shows the Bode plots of log (Z") to log (f) at different voltages.

It can be seen from Fig. 4 and 6 that the ac impedance of the SLED is voltage dependent. When the bias voltage is lower than 3 V, such as at 2 V, the impedance is very similar to that at 0 V, except that the straight line in the lower frequency range is bent a little (R_2 decreased a little). However, when the bias voltage is equal to, or higher than 3 V, the impedance plots changed dramatically. At 3 V the straight line in the lower frequency range moved upward, and at 4 V it moved to the straight line. The latter almost overlapped to the straight line in the higher frequency range, which means that C_2 decreased with an increase in bias voltage and it closes to C_1 after the voltage is higher than 4 V. The voltage dependence of R_2 is interesting. It decreases with increasing voltage when the voltage is lower than 4 V. Then it changes to increase with increasing voltage from 4 V to 6 V, as shown in Fig. 6.

SLED involves electrochemical reaction at the interface between the electrode and the polymer solution. ITO was used as both the anode and the cathode. A chemical reaction of ITO (ITO become black) was observed at the cathode interface. Different coatings on the ITO electrode and aluminum electrode were examined to improve the device performance. PEDOT, a well-known hole-injection material, and LiF were placed on top of the ITO electrodes as a bilayer anode and cathode, respectively. Better charge injection and device performance were observed. (Fig.7a and 7b) Using metal electrodes rather than ITO also resulted in better device performance. (Fig. 8a and 8b).

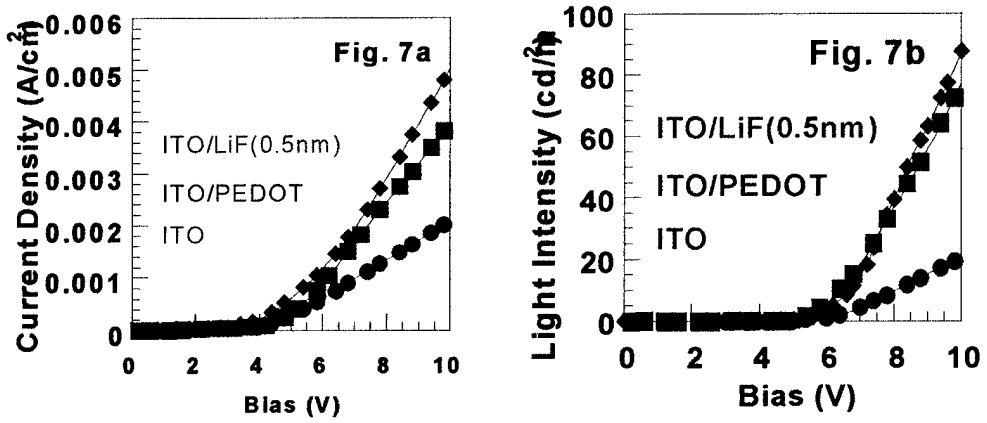

Fig. 7a and 7b show the I-V and L-V curves, respectively, of SLED under the different bilayer electrodes as well as the bare ITO.

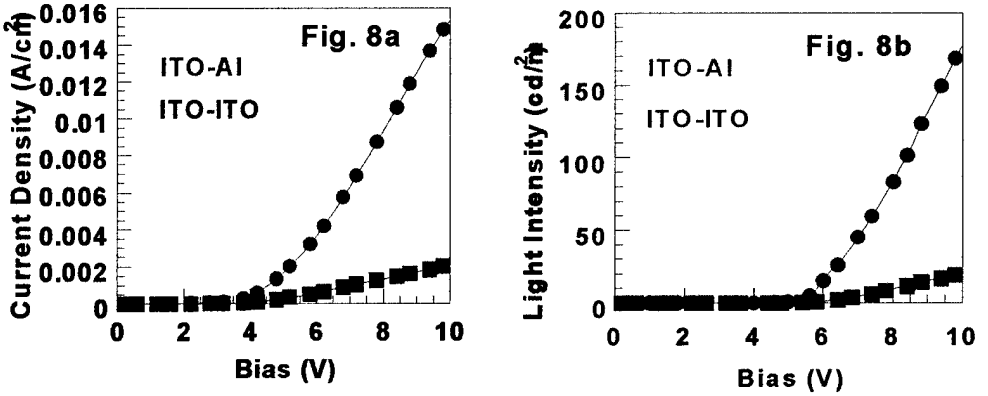

Fig 8a and 8b show the I-V and L-V curves of SLED using Al as a cathode in comparison to SLED using the ITO as the anode as well as cathode.

Laminated Polymer LED (Second Year)

In the second year of this project, we have expanded the study of SLED into the solid LED by inventing the low temperature lamination process. We have achieved a breakthrough in laminated polymer LED.

Firstly, we created the template activated surface (TAS) process for a low temperature plastic lamination. Our laminated device consists of the two components: the anode part and the cathode part. The anode-part contains the anode on a substrate and a polymer (or organic) layer, which can be either a hole-transport layer or a luminescent polymer. For the cathode part, it was generated by using an adhesive strip to lift off the polymer film with thermally evaporated metal electrode from the indium-tin-oxide /glass (ITO/glass) substrate. This is what we named TAS process, because the lifted-off polymer surface reflects the mirror imagine of the ITO. The evidence for this activated interface had been further characterized through the analysis of atomic force microscopy (AFM) and contact angle measurement. **Through this unique activated process, two pieces of polymer/electrode film can be laminated together to become an electronic device. This lamination process is carried out at ~60 °C; this is rather low temperature compares to the traditional polymer lamination process, typically requires a temperature higher than 100C.**

Secondly, the applying of this TAS approach for the fabrication of laminated PLED shows a very promising result. MEH-PPV was first chosen as the luminescent material to demonstrate the laminated device. The total thickness of the active layer in the laminated device was around 900 Å, which is close to the thickness of the active layer in a single-layer device. The I-L-V curves are shown in Figure 9. The charge injection occurs at 1.6 V, and the device turned on below 2 V. This is consistent with the device characteristic using traditional fabrication methods. The electroluminescence (EL) spectrum of this device, as shown in Figure 10is similar to that of the single-layer device. The efficiency of the laminated devices can be as high as 0.34 cd/A at 6 V with a rectification ratio of 10^5. The illumination of the laminated PLED, as shown in the inset of Figure 2, was found to be uniform across the device as examined by optical microscopy. This indicates that the charge injection and recombination occurred within the whole pixel and that the properties of the interface are uniform across the device. **We**

are proud to present this result to AFOSR the first successful demonstration of laminated PLED.

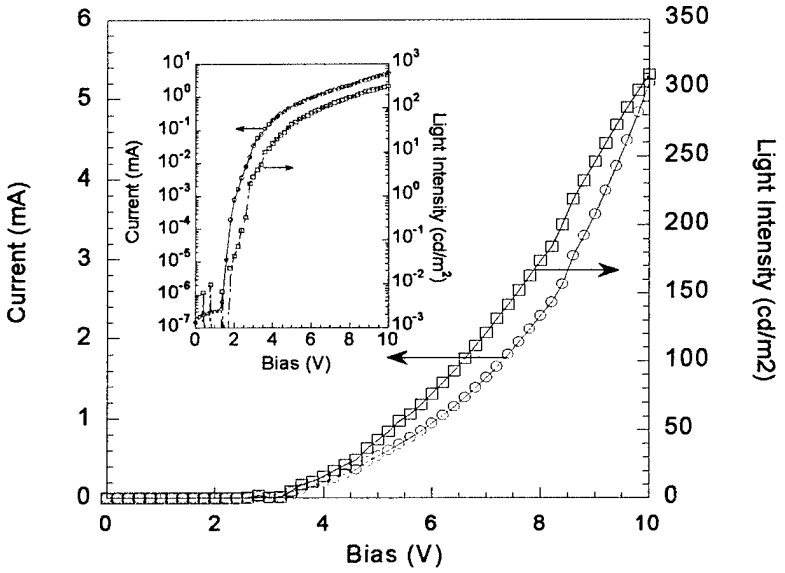

Fig. 9 The I-L-V cures of the laminated PLED. The insert shows the logarithm scale of the I-L-V curve. The device area is ca. 0.04 cm^2.

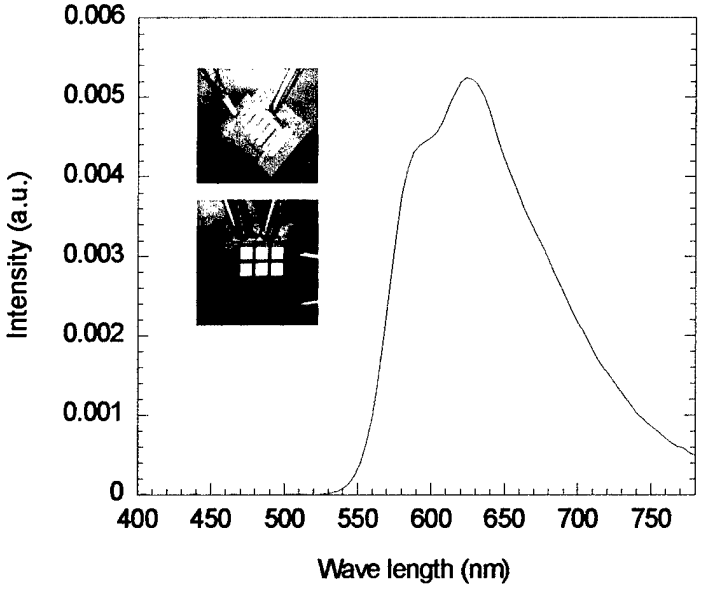

Fig. 10 Electroluminescence spectrum and photographs of MEH-PPV-based laminated PLED. Upper insert shows a uniform single pixel, and bottom insert is a 2x3 X-Y based passive device.

High performance polymer LEDs and LECs (The third year)

Due to the harvest of singlet and triplet excitons, considerably high quantum efficiency has been achieved in phosphorescent PLEDs. However, in highly-doped PLEDs (usually > 1% wt), the driving voltage increases because of carrier trapping at the dopant. The build-up of space charges further hinders the injection of carriers and, subsequently, increases the turn-on voltage and the device operating voltage. As a result, the power efficiencies of the phosphorescent PLEDs are still low; despite high quantum efficiencies that have been demonstrated. Light-emitting electrochemical cells (LECs) usually have very low driving voltage, thus they provide an alterative way to achieve high power efficiency.

Phosphorescent LECs were fabricated by spin-coating a polymer blend, consisting of BDOH-PF, lithium triflate ($LiCF_3SO_3$) and a phosphorescent dopant, bis(2-(2'-benzothienyl)-pyridinato-N,$C^{3'}$)iridium (acetylacetonate) (BtpIr), from cyclohexanone onto a pre-cleaned indium-tin-oxide (ITO) substrate. The weight ratio of the polymer thin films was BDOH-PF:$LiCF_3SO_3$:BtpIr = 1:0.1:0.05 (defined as device A). Fig. 11 shows the time-dependent current-brightness curves for the device A biased at 3.5V. The device turned on slowly and emitted red light. The slowly increasing current and emission intensity was probably due to the formation of *p*-type and *n*-type doped regions near the electrodes. The device turn-on speed increased with higher bias voltage. The highest quantum efficiency achieved was 1.2 cd/A. The inset in Fig. 11 illustrates the power efficiency as a function of operating time. The power efficiency increased initially and reached a maximum of 1.0 lm/W, at the brightness of 0.2 cd/m^2. At the highest brightness, 16 cd/m^2, the power efficiency was about 0.30 lm/W.

The PL and EL spectra of device A were also obtained (Fig. 12). The EL exhibited solely red emission with a maximum wavelength of 616 nm and the spectrum was consistent with the PL of BtpIr in a dilute solution, which suggests that the emission indeed came from the triplet state of the dopants. On the other hand, the PL of the device A came from the host (BDOH-PF) as well as the dopant (BtpIr), implying incomplete energy transfer. The different between PL and EL suggests that the carrier trapping occurred while the device was operated. It indicates that the direct recombination of electrons and holes in the dopant is one of the main mechanisms of our dye-doped LECs.

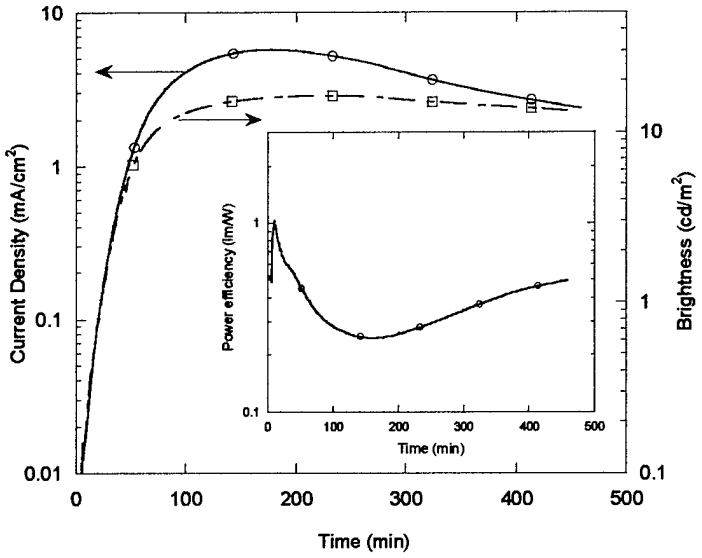

Figure 11: The time-dependent I-L-T curves of device A; device structure was ITO/BDOH-PF:LiCF$_3$SO$_3$:BtpIr/Al. The inset shows the time-dependent device-efficiency.

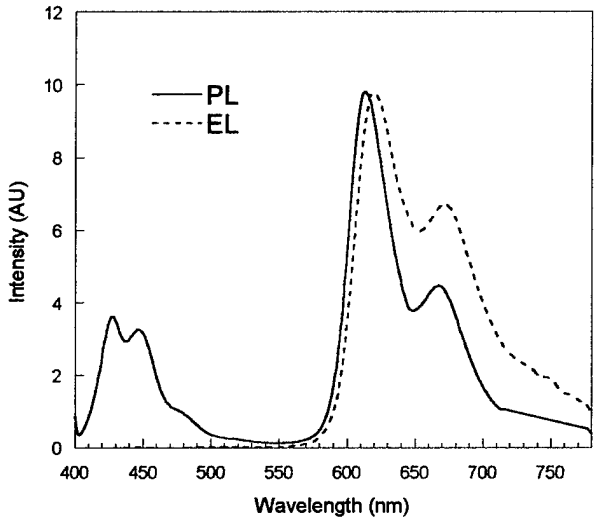

Figure 12: The PL (the solid line) and EL (the dashed line) spectra of device A.

For comparison, we also fabricated conventional PLEDs based on the same materials *without* the addition of salts and PEO. The device structure is as follows: ITO/BDOH-PF:BtpIr (1:0.05)/Al. The light turn-on voltage was found to be around 12.1 V and the highest quantum efficiency was 1.0 cd/A. The highest power efficiency was 0.16 lm/W at 40 cd/m^2. Comparing

with the power efficiencies of device A with this LED, ca. six-fold enhancement has been achieved in the LEC device by adding salts.

Triplet sensitizer for efficient PLED:

In parallel to lowering the operating voltage, we also demonstrated a general method to enhance the quantum efficiency of conventional fluorescent PLEDs by incorporating a phosphorescent dye into the emissive layer as a sensitizer. The function of the phosphorescent sensitizer is to convert the triplet exciton into singlet exciton during the energy transfer process.

Poly (9-vinylcarbazole) (PVK; M_w ~1,100,000g/mol) was selected as the host material (and the hole-transport material), and 2-(4-biphenylyl)-5-(4-*tert*-butyl-phenyl)-1,3,4-oxadiazole (PBD) as the electron-transport molecule. The phosphorescent dye, *bis*(2-phenyl pyridinato-$N,C^{2'}$) iridium (acetylacetonate) (PPIr) was used as the sensitizer. Fluorescent dyes - Alq_3 and Nile Red, were dissolved in DCB and then mixed at various ratios with the host materials and PPIr to achieve appropriate weight percentages. The mixed solution was passed through 0.45μm filters before spin-coating. The device structure was ITO/3,4-polyethylenedioxythiophene-polystyrenesulfonate (PEDOT) / PVK(PBD) + 1%PPIr + 1% Nile Red/Ca/Al.

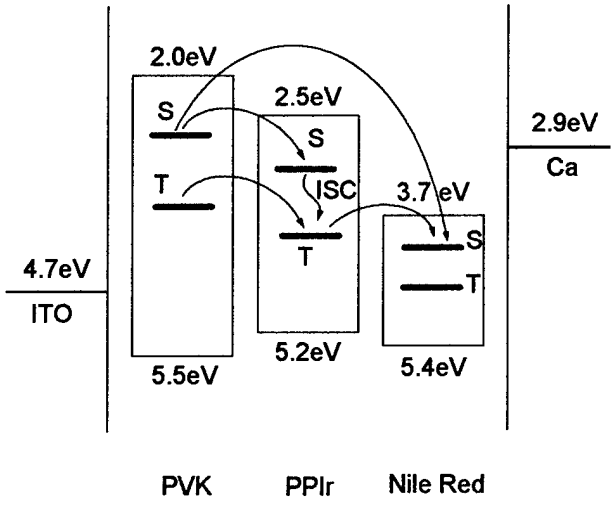

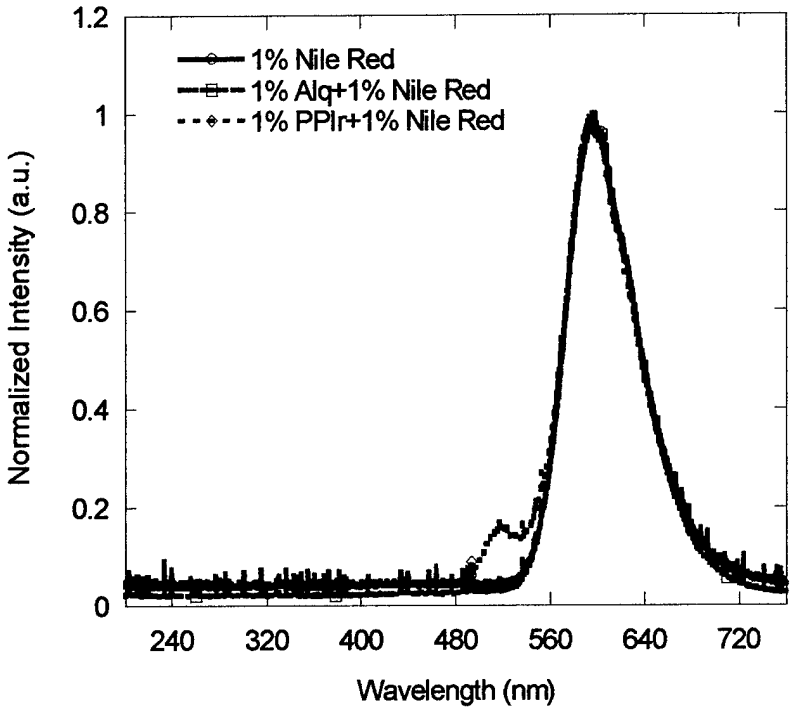

Figure 13: The EL spectra of the devices. Inset: Energy diagram and proposed energy transfer mechanism.

A possible energy transfer mechanism is proposed (inset of Figure 3) for this system. After the injection of electrons and holes from the cathode and the anode respectively, the excitons are formed in the host material PVK with a ratio of 25% singlets to 75% triplets. Then the singlet excitons and the triplet excitons are transferred to the singlet states and the triplet states on PPIr by a combination of Förster and Dexter processes along with carrier trapping. Within PPIr, the singlet excitons transfer to the triplet states through the intersystem crossing (ISC) process. Because of the presence of Nile Red dopant, the triplet excitons in PPIr can transfer to the singlet exciton in Nile Red through Förster transfer by dipole-dipole coupling. The Nile Red singlets then decay radiatively and give out light.

To verify the proposed energy transfer mechanism, two controlled devices were fabricated: ITO/PEDOT/PVK(PBD)+1%Nile Red/Ca/Al and ITO/PEDOT/PVK(PBD) +1%Alq_3+1%Nile Red/Ca/Al. Alq_3 was used for comparison because Alq_3 and PPIr are both green-emitting materials and have similar spectra except that Alq_3 is a fluorescent dye while PPIr is a phosphorescent dye. Fig. 13 shows the EL spectra for these two devices. That there is no host

emission observed for both cases indicates full energy transfer from the host to the fluorescent dyes. The host singlet excitons are transfered to both fluorescent sensitizer singlet states and fluorescent dye by Förster process. Having given the energy from PVK host, Alq_3 singlets would rather transfer the energy to Nile Red again than decay to their ground states directly, as there exists a good overlap between Alq_3 emission and Nile Red absorption. Hence, Alq_3 emission was not shown on the EL spectrum of the device using PVK(PBD):Alq_3:Nile Red blend as the active materials.

Fig. 14 shows the current efficiency vs. current density curves for these devices. The efficiency of ITO/PEDOT/PVK(PBD)+1%Nile Red/Ca/Al device is about 2.2 cd/A. When another fluorescent dye Alq_3 was added to the system, the efficiency of the device remains almost unchanged. On the other hand, dramatic enhancement of EL efficiency (6.7 cd/A) was observed after adding phosphorescent PPIr. PPIr was used just like a sensitizer, which harvests both singlets and triplets of the host and then transfers them to fluorescent dye. The efficiency of this device was two times than that of the controlled devices.

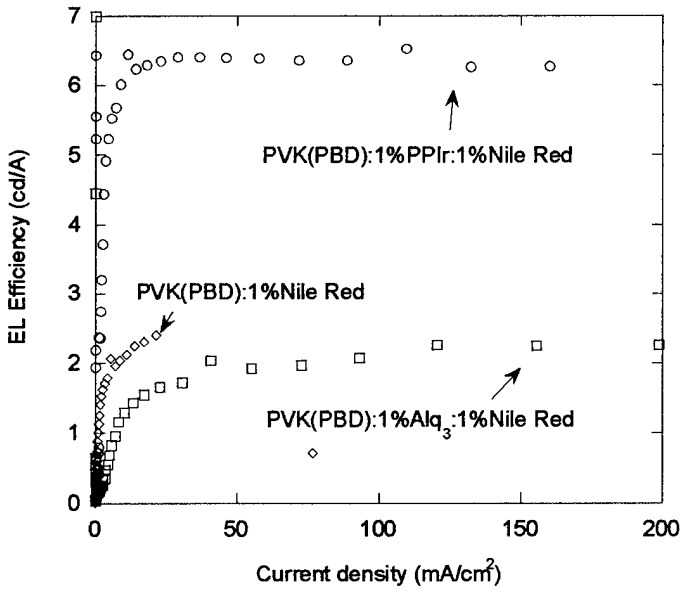

Figure 14. EL efficiency (cd/A) of the devices in different structure vs current density.

High performance polymer photovoltaic cells

In the third year, a breakthrough has been achieved at UCLA, which significantly enhances the *Isc* of the plastic PV cells. The PV process contains four major steps, which are as follows: absorption of photons, generation of electron-hole pairs, dissociation of the e-h pairs, and finally, collection of charges. For polymer PV cells, the major bottleneck is the charge collection, which is hindered by low carrier mobility and conductivity. Our invention is aimed towards the enhancement of the conductivity/mobility at the last stage of PV process. It is known that by adding a small amount of electrolyte to the conjugated polymer, the carrier mobility (or conductivity) can be significantly improved. However, precautions need to taken to avoid the enhancement of undesirable dark current.

By adding a very small amount of ionic electrolyte into the plastic PV cells, we discovered that the *Isc* was doubled. The device structure is a typical polymer solar cell, consisting of a layer of polymer thin film sandwiched between a transparent anode (indium tin-oxide, ITO) and a cathode. The active material is an admixture of poly(2-methoxy-5-(2'-ethyl-hexyloxy)-1,4-phenylene vinylene)] (MEH-PPV, a p-type polymer) and C_{60} (a n-type electron acceptor).

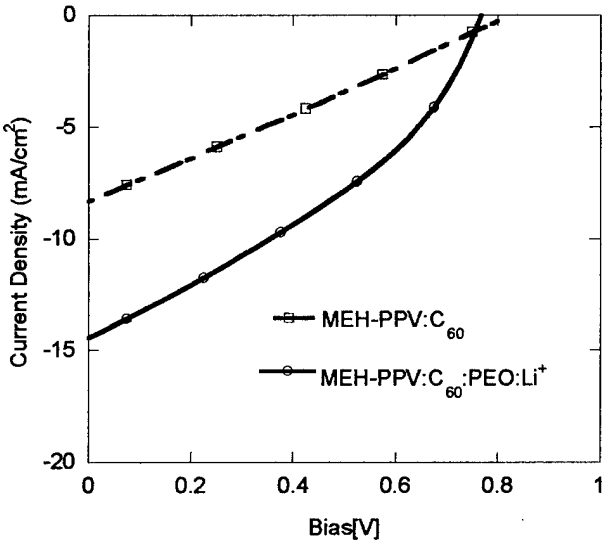

Figure 15. The I-V curves of MEH-PPV:C_{60} devices with and with adding polymer electrolyte under 120 mW/cm^2 white illumination. Device structure: TO/PEDOT/active polymer layer/Ca/Al.

Fig. 15 shows the I-V curves of MEH-PPV: C_{60} devices without (Device I) and with (Device II) solid electrolyte under 120 mW/cm^2 white light illumination from the transparent indium tin-oxide (ITO) anode. The open-circle voltage (Voc) and the short-current density (*Isc*) of Device I are 0.83 V and 8.3 mA/cm^2, respectively. The fill factor (FF), which is defined as the maximum power $(IV)_{max}$ divided by the product of Voc and *Isc*, is around 0.26. The power conversion energy is thus calculated as 1.5%. After adding the polymer electrolyte, where the weight ratio of active polymer layer is MEH-PPV:C_{60}:PEO:$LiCF_3SO_3$ = 3:1:0.25:0.05, it can be clearly seen that the *Isc* of Device II increases to 14.4 mA/cm^2. The fill factor was increased from 0.26 to 0.36, a 38% increase. The higher FF and power conversion efficiency indicate that adding ionic electrolyte has improved the device performance.

The effect of the concentration of PEO/Li^+ in the active polymer blend on the *Isc* is illustrated in Fig. 16. The *Isc* increases initially with the amount of PEO/Li^+ and then goes down while more electrolyte is added. The optimized PEO concentration is thus found to be around 20wt% of C_{60}, which corresponds to 6.7 wt% of MEH-PPV. Meanwhile, Voc decreases with the increasing amount of ionic electrolyte and drops to 0.75V at 90% PEO/Li^+.

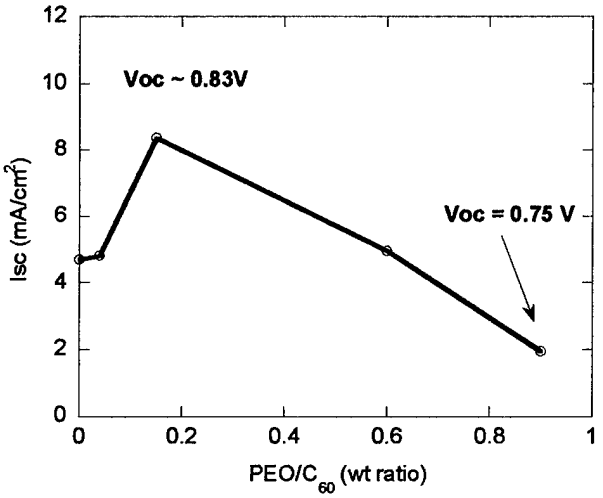

Figure 16. The short-circuit currents of devices with different amount polymer electrolyte under 80 mW/cm^2 white light illumination.

The reason for this efficiency improvement is still unclear. The improvement of charge transportation in the polymer layers and/or stabilization of the charge-separation states by

changing the dielectric environment are some of the possibilities. This will be one of our research focuses in the future.

Publications

SLEDs:

1. Shun-Chi Chang, Yang Yang, Fred Wudl, Yongfang Li, "AC impedance characteristics and modeling of polymer solution light-emitting devices", J. Chem. Phys., 105, 11419-11423 **(2001)**
2. Shun-Chi Chang, Gufeng He, Fang-Chung Chen, Tzung-fang Guo, and Yang Yang, "Degradation mechanism of polymer light-emitting diodes based on phosphorescent dyes", Appl. Phys. Lett., 79, 2088, **(2001)**.
3. Shun-Chi Chang, Yongfang Li, and Yang Yang, "Electro-generated chemiluminescence mechanism of polymer solution light emitting devices", J. Phys. Chem., 104, 11650 **(2000)**.
4. Gufeng He, Shun-Chi Chang, Fang-Chung Chen, Yongfang Li, and Yang Yang, "Highly efficient polymer light-emitting devices using a phosphorescent sensitizer", 81, 1509, **(2002)**.

PLEDs

5. Tzung-Fang Guo, Seungmoon Pyo, Shun-Chi Chang, and Yang Yang, "High Performance Polymer Light-Emitting Diodes Fabricated by A Low Temperature Lamination Process", Advanced Functional Materials, 11, No. 5, 339, **(2001)**.
6. Shun-Chi Chang, Gufeng He, Fang-Chung Chen, Tzung-fang Guo, and Yang Yang, "Degradation mechanism of polymer light-emitting diodes based on phosphorescent dyes", Appl. Phys. Lett., 79, 2088, **(2001)**.
7. Tzung-Fang Guo, Gufeng He, Seungmoon Pyo, and Yang Yang, "Investigation of the interfacial properties of laminated polymer diodes", Appl. Phys. Lett. 80, 148, **(2002)**.
8. Jianyong Ouyang, Tzung-Fang Guo, Jie Liu, Yang Yang, "High-performance flexible polymer light-emitting diodes fabricated by a continuous polymer coating process", Adv. Materials, 14, 915, **(2002)**.
9. Fang-Chung Chen and Yang Yang, "High-performance polymer light-emitting diodes doped with a red phosphorescence Ir complex", Appl. Phys. Lett., 80, 2308, **(2002)**.

PV:

One PV paper is still under preparation, a patent was filed.